1992-06

Slow Speed Flight Control of Autonomous Underwater Vehicles: Experimental Results with NPS AUV II

Healey, A.J.

The International Society of Offshore and Polar Engineers

Proceedings of the Second (1992) International Offshore and Polar Engineering Conference
San Francisco, USA, 14-19 June 1992

ISBN 1-880653-00-1 (Set); ISBN 1-880653-02-8 (Vol II)

SLOW SPEED FLIGHT CONTROL OF AUTONOMOUS UNDERWATER VEHICLES: EXPERIMENTAL RESULTS WITH NPS AUV II

A.J. Healey and D.B. Marco
Naval Postgraduate School
Monterey, California, USA

ABSTRACT

A six degree of freedom model for the maneuvering of an underwater vehicle is discussed in which the hydrodynamic force coefficients are scaled from previous studies of a Swimmer Delivery Vehicle, and traditional as well as Sliding Mode controllers are designed for the steering, diving, and speed control functions. In slow speed flight control applications of this kind, difficulties arise because the system to be controlled is highly non-linear, coupled, and there is a good deal of parameter variation with operational conditions. The uncertainty in force coefficients and disturbances make control difficult. This paper presents an outline of the controller design methodology, a description of the testbed vehicle and a discussion of experimental flight control results for way point following, bottom following, and sonar mapping of the surrounding environment. It shows that a multivariable autopilot based on state feedback, designed assuming decoupled modeling, is quite satisfactory for the combined speed, steering and diving response of a slow speed AUV enabling autonomous missions to be planned.

INTRODUCTION

This paper proposes the use of a multivariable sliding mode autopilot for the combined control of AUV steering, depth and speed during complex slow speed flight maneuvers. The method draws upon the the power of sliding modes to reduce the inherent coupling between the vehicle response modes that naturally exist in ROV / AUV vehicles. The approach leads to a set of separate designs for steering, diving and speed control systems, which is often the case in flight vehicles, and this paper provides experimental results using a testbed vehicle that illustrate the performance of the controllers used.

Well behaved autopilot systems enable the use of a variety of guidance schemes to achieve way point and path tracking. Vehicle guidance is illustrated using proportional line of sight guidance. Experimental results with the NPS AUV II vehicle show that way point following, bottom following and sonar mapping of the surrounding environment are possible.

The paper contains a discussion of the vehicle modeling, the control design and guidance scheme, and the results of motion control experiments with the testbed vehicle.

BACKGROUND

The design of an autopilot for the motion control of underwater vehicles is of interest both from the view of motion stabilization as well as maneuvering and tracking performance. AUV's of the class considered here, fall between the two extremes of unmanned underwater vehicles, (the ROV's and the TORPEDO type), and are difficult to control having highly variable and uncertain dynamics. Recent work concerned with the modeling and control of ROV vehicles includes Lewis, Lipscomb and Thompson (1984) who described an ROV simulation program using linear hydrodynamic coefficients. ROV vehicles do not possess hydrodynamically shaped profiles and the hydrodynamic forces are uncertain and difficult to predict (Dand and Every, 1983). To overcome the widely varying and uncertain behavior of these vehicles Russel and Bugge (1981) had considered the use of an adaptive automatic guidance system including modeling strong measurement noise of uncertain spectral nature. Yoerger and Slotine (1985, 1986) proposed and successfully used a sliding mode controller for an ROV maneuvering around large objects at very slow speed; and Goheen, Jefferys and Broome (1987), described a "self testing" procedure for evaluation of the vehicle dynamic response and a corresponding automatic gain selection. The work of Yoerger and Slotine with robust control using sliding modes is most encouraging, and, although the extra time taken to perform the self-test of Goheen et. al. may not always be available, it still has merit. Recently, Yoerger et. al., (1991) have shown that the dynamics of torque controlled thruster elements are problematic in ROV positioning because lags in the thrust response, if not taken into account, can lead to vehicle limit cycling behavior. Fossen(1991) describes the use of multivariable sliding mode control in dynamic positioning of ROV's with simulations.

For higher speed vehicles than ROV's, and those with more streamlined hydrodynamic characteristics, the situation is different and previous work has been reported by Lindgren, et. al., (1967) who addressed the issues of steering and depth control of a torpedo, pointing out the importance of the non-linear hydrodynamic behavior and the stroke limits of the surfaces; Young (1969), described the stability derivatives of the Navy's DSRV vehicle, and Smith et. al. (1978) gave a comparison of the performance of a simulator for a Swimmer Delivery Vehicle with

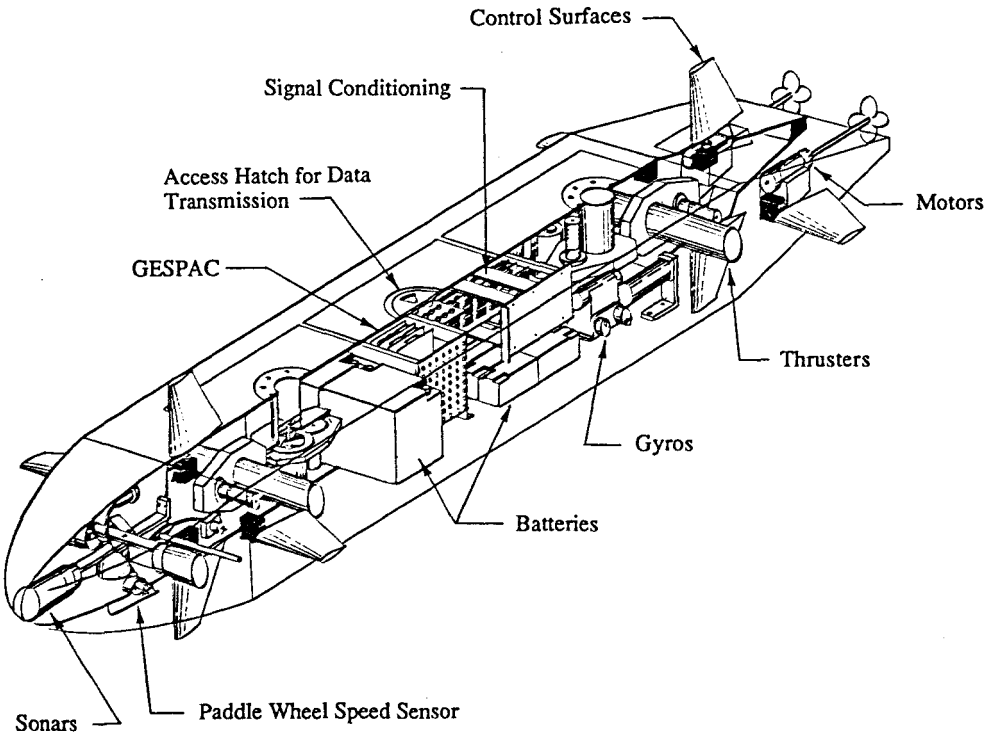

Figure 1
Sketch of the NPS AUV II Autonomous Underwater Vehicle

field response data, as well as Dobeck et. al. (1982), who provided an unclassified description of tests conducted on the Control Systems Test Vehicle (CSTV) under closed loop computer controlled maneuvering. Humphries (1981) describes analytical and empirical considerations for the evaluation of hydrodynamic coefficients while Gueler (1989) studied the independent use of bow and stern planes in submarine depth control under the action of wave forces. Richards and Stoten (1981), modeling the disturbance response to waves, and later Milliken (1984), concerned about the yaw-pitch coupling during turns, applied a linear model based compensator to the problem of depth control. Optimized trade-offs between plane action and the depth error response in waves is possible. So far, the issues of robustness had not been addressed to the same degree as for the ROV vehicles. Milliken, described the use of a linearized model-based compensator to reduce the pitch-yaw coupling during turns for a linear submarine vehicle in which a full-state observer was employed in the compensator. Some reduction in pitch induced response was achieved depending on speed. A gain schedule with two separate speed regimes was proposed. Consideration was given neither to the design of a command generator nor the feedforward response shaping for depth changing maneuvers. Recently, however, Ruth and Humphreys (1990) have discussed the use of robust control design using μ synthesis methods for the coupled speed / depth control of a heavy UUV at slow speed. In this case the plane action must balance the vertical loading forces at different speeds, which affects the depth response. Simulation results indicated that a classical controller could be improved using the 10 state compensator described. Dougherty and Woolweaver (1990) have also shown that a mixed sliding mode control with an inner pitch control and outer depth control loop as used on the MUST vehicle provides satisfactory coupled behavior, although the details of the control design are few. Others have suggested the use of sliding modes with adaptivity, as in Cristi et. al. (1991) for depth control, where the sliding surface is based on system state and state estimators rather than on output error.

It is the robustness of control of UUV's which will typically operate in the range of 0-15 knots that needs to be addressed, and is the subject of this work. While many theory and simulation papers abound, few have provided details of results from working systems as in the case presented here.

VEHICLE MODELING

The three-dimensional equations of motion for hydrodynamically shaped underwater vehicles have been described in general terms by Abkowitz (1969), and are most conveniently developed using a body-fixed coordinate frame and a global reference frame. The body-fixed frame has components of motion given by the six velocity components, [u(t),v(t),w(t),p(t),q(t),r(t),] relative to a constant velocity coordinate frame moving with the ocean current, $\mathbf{u}_c$, and the velocity vector is represented as,

$$\mathbf{x}'(t) = [u(t), v(t), w(t), p(t), q(t), r(t)] \quad (1)$$

while the six components of position in the global reference frame are,

$$\mathbf{z}'(t) = [X(t), Y(t), Z(t), \phi(t), \theta(t), \psi(t)] \quad (2)$$

The angles $\psi(t)$, $\theta(t)$, $\phi(t)$, (azimuth, elevation, and spin), are related here through Euler transformations to the body yaw, pitch, and roll motions. Control inputs from control surfaces, propeller speeds, thruster forces and buoyancy adjustment in general may be considered as the vector, $\mathbf{u}(t)$. For the case at hand, eight control surfaces are combined to form a steering control, a diving control, and a speed control and the vehicle is assumed to be neutrally buoyant with no active buoyancy or roll control present at this time. Specifically, $\mathbf{u}(t)$ is given by,

$$\mathbf{u}(t)=[\delta_r(t), \delta_s(t), n(t)] \quad (3)$$

The development of the functional form of the hydrodynamic forces has been well studied and, in terms of first order variations of motion components, were given by Gertler and Hagen, (1967), and later by Abkowitz. Specific values of the particular coefficients depend on specific vehicles, although normalization by speed and length can provide some generalized feeling as to their scaling behavior. The values used in this work were based on scaled values from the Swimmer Delivery Vehicle, a box shaped vehicle (Smith et. al., 1978), somewhat similar to the NPS AUV II vehicle outlined in Figure 1. The functional form of the force equations are given in Healey, (1992). The SDV model includes, a model of the cross flow drag effects and a model of the propulsion system and is therefore a large departure from the original work of Abkowitz although the cross flow drag terms have been neglected in the modeling used for the NPS AUV II.

The vehicle motion may be described in terms of the twelve non-linear system equations,

$$\mathbf{M}(t)\,\dot{\mathbf{x}}(t) = \mathbf{f}(\mathbf{x}(t),\mathbf{z}(t),\mathbf{c}(t)) + \mathbf{g}(\mathbf{x}(t),\mathbf{z}(t))\,\mathbf{u}(t)$$

$$\dot{\mathbf{z}}(t) = \mathbf{h}(\mathbf{z}(t),\mathbf{x}(t),\mathbf{u}_c) \qquad (4)$$

in which the coupled mass matrix $\mathbf{M}(t)$, includes both mechanical and hydrodynamic added mass; the functions $\mathbf{f}$ are mappings of the vehicle motions into forces, including coriolis, gravitational, and centrifugal forces; the hydrostatic and hydrodynamic forces and moments acting on the vehicle in the body fixed coordinate frame, with coefficients $\mathbf{c}$. Functions $\mathbf{g}$ represent the motion dependent influence of control surface, thruster, and any ballasting inputs. The functions $\mathbf{h}$ include the kinematical relationships found in performing the needed coordinate transformations between body fixed and global reference frames and the constant ocean current, $\mathbf{u}_c$ assumed to be negligible here.

Once a hydrodynamic design is made, these functions can be estimated and are known through vehicle dynamic modeling to lie within a finite bound where that bound can be established, a priori, if knowledge of the variability of the vehicle coefficients, $\mathbf{c}$ is assumed. The functions $\mathbf{f}$ and $\mathbf{g}$ are known to be finite gain stable. Using the Euler angle approach, $\mathbf{h}$ is known to be finite gain stable everywhere except at the point where $\theta(t) = \pi/2$. In this situation and with equations (4) as the background model for a general underwater vehicle during maneuvering, the concept of a multivariable sliding mode control will be developed.

SLIDING MODE CONCEPTS

We define sliding surfaces in the state error space with the object of finding a sufficient relationship for each of the control element inputs $\mathbf{u}(t)$ that will guarantee global asymptotic stability of the state variable errors and provide adequate performance under closed loop conditions. To this end, we define a sliding surface so that each passes through the origin of the state error space. State errors are defined by:

$$\begin{bmatrix}\tilde{\mathbf{x}}(t)\\ \tilde{\mathbf{z}}(t)\end{bmatrix} = \begin{bmatrix}\mathbf{x}(t)\\ \mathbf{z}(t)\end{bmatrix} - \begin{bmatrix}\mathbf{x}(t)\\ \mathbf{z}(t)\end{bmatrix}_{com} \qquad (6)$$

where the commands are derived from a consistent command generation system , or planned path, or from a series of way points corresponding to desired values of vehicle velocity or position (posture) as appropriate. The set of sliding surfaces in the error space are then:

$$\sigma(\tilde{\mathbf{x}}(t),\tilde{\mathbf{z}}(t)) = \begin{bmatrix}\mathbf{S}_1 & \mathbf{S}_2\end{bmatrix}\begin{bmatrix}\tilde{\mathbf{x}}(t)\\ \tilde{\mathbf{z}}(t)\end{bmatrix} \qquad (7)$$

where, $\sigma(t) \in \Re^{6\times 1}$; $\mathbf{S}_1, \mathbf{S}_2 \in \Re^{6\times 6}$;

Notice that in this work as opposed to the work of Slotine and Yoerger (1985), the sliding surface is based on state variable errors rather than output errors. For flight vehicles in which the modes are highly coupled, we find this approach to be more flexible. The coefficients $\mathbf{S}_1$ and $\mathbf{S}_2$ are assumed to be known at this point in the development, although as will be seen, are not arbitrary. In fact, system closed loop response is dependent on values selected, and at least part of any design procedure using sliding mode methods is to properly select surfaces having stable eigenvalues so that stable sliding modes will exist, namely that for all t and $[\mathbf{x}(t), \mathbf{z}(t)]$ lying in the space of maneuvers to be accomplished, the condition :

$$\dot{\sigma}(\tilde{\mathbf{x}}(t),\tilde{\mathbf{z}}(t)) \to 0 \text{ as } t \to \infty$$

with

$$\sigma(\tilde{\mathbf{x}}(t),\tilde{\mathbf{z}}(t)) \to 0 \text{ as } t \to \infty \qquad (8)$$

will also imply

$$\tilde{\mathbf{x}}(t),\ \tilde{\mathbf{z}}(t) \to 0 \quad \text{as } t \to \infty \qquad (9)$$

and stable tracking behavior can be achieved. Global asymptotic stability of the tracking error is guaranteed by the sliding condition, (8) through consideration of $\sigma(\tilde{\mathbf{x}}(t),\tilde{\mathbf{z}}(t))$ in terms of a Lyapunov function $V(t)$, yields,

$$V(t) = 0.5\ \sigma'(\tilde{\mathbf{x}}(t),\tilde{\mathbf{z}}(t)) * \sigma(\tilde{\mathbf{x}}(t),\tilde{\mathbf{z}}(t))$$

so that for global asymptotic stability,

$$\frac{dV}{dt} = \dot{\sigma}'(\tilde{\mathbf{x}}(t),\tilde{\mathbf{z}}(t)) * \sigma(\tilde{\mathbf{x}}(t),\tilde{\mathbf{z}}(t)) \ < 0 \qquad \forall\ t\ > 0$$

If we define positive functions $\eta_i(t)$ then it may be shown that a candidate switching relationship which guarantees stability for each $\sigma_i(t)$ may be chosen as in

$$\dot{\sigma}_i(\tilde{\mathbf{x}}(t),\tilde{\mathbf{z}}(t)) = -\eta_i(t)\ \mathrm{sgn}(\sigma(\tilde{\mathbf{x}}(t),\tilde{\mathbf{z}}(t)))\ \ i = 1,\ldots,6$$

We find it better, in fact, to use a continuous function to define the sliding condition which is given by,

$$\dot{\sigma}_i(\tilde{\mathbf{x}}(t),\tilde{\mathbf{z}}(t)) = -\eta_i(t)\tanh(\sigma_i(\tilde{\mathbf{x}}(t),\tilde{\mathbf{z}}(t))/\phi_i) \qquad (10)$$

The powerful result of equation (10) means that if the $\eta_i(t)$ are large enough, then in spite of modeling uncertainty, non-linear terms, and disturbances, the system response will be governed by the response of the $\sigma_i(t)$ and by the choice of the sliding surface parameters: it is less influenced by the parameters of the vehicle dynamics as is more usual with linear feedback controllers. The ϕ_i, not to be confused with the vehicle's roll motion Euler angle, $\phi(t)$, are sliding surface boundary layer parameters used to retain continuity of control as motion trajectories cross the sliding surface.

Assuming that $\mathbf{S}_{1,2}$ are established (by the method to be described here), substitution of equations (2) and (3) into (10) yields a solution for the control law and using 'best estimates' of the functionals in the vehicle motion equation gives,

$$\begin{aligned}&\mathbf{S}_1\left\{\mathbf{M}^{-1}(t)\left[\mathbf{f}(\mathbf{x}(t),\mathbf{z}(t),\mathbf{c}(t)) + \mathbf{g}(\mathbf{x}(t),\mathbf{z}(t))\mathbf{u}(t)\right] - \dot{\mathbf{x}}(t)_{com}\right\}\\ &+\mathbf{S}_2\left\{\mathbf{h}(\mathbf{z}(t),\mathbf{x}(t),\mathbf{u}_c) - \dot{\mathbf{z}}(t)_{com}\right\} = -\mathbf{F}(\sigma,\phi)\end{aligned} \qquad (11)$$

Since the $\mathbf{f}(\cdot)$, $\mathbf{g}(\cdot)$, and $\mathbf{h}(\cdot)$ are uncertain in general, we use the

estimates, $\hat{\mathbf{f}}(\cdot),\hat{\mathbf{g}}(\cdot),\hat{\mathbf{h}}(\cdot)$, with which the solution for $\mathbf{u}(t)$ follows as

$$\mathbf{u}(t) = \mathbf{u}_1+\mathbf{u}_2+\mathbf{u}_3$$

where;

$$\mathbf{u}_1 = [\hat{\mathbf{g}}(\mathbf{x}(t),\mathbf{z}(t))]^{-1}[\{\mathbf{S}_1\mathbf{M}^{-1}\}^{-1}\dot{\mathbf{x}}(t)_{com} - \hat{\mathbf{f}}(\mathbf{x}(t),\mathbf{z}(t),\mathbf{c}(t))]$$

$$\mathbf{u}_2 = [\hat{\mathbf{g}}(\mathbf{x}(t),\mathbf{z}(t))]^{-1}\{\mathbf{S}_1\mathbf{M}^{-1}(t)\}^{-1}\mathbf{S}_2[\dot{\mathbf{z}}(t)_{com} - \hat{\mathbf{h}}(\mathbf{z}(t),\mathbf{x}(t),\mathbf{u}_c)]$$

$$\mathbf{u}_3 = -[\hat{\mathbf{g}}(\mathbf{x}(t),\mathbf{z}(t))]^{-1}\{\mathbf{S}_1\mathbf{M}^{-1}(t)\}^{-1}\mathbf{F}(\sigma,\phi) \qquad (12)$$

and the right hand side of (10) become the elements of the column vector $\mathbf{F}(\sigma, \phi)$.

The control $\mathbf{u}_1$ balances the estimates of the forces to perform the required maneuver, $\mathbf{u}_2$ provides stabilization based on estimates of the positional elements in $\mathbf{h}$, and the current, and $\mathbf{u}_3$ is a switching term that drives the state to the sliding surface.

Equation (12) shows a useful structure provided $\mathbf{S}_1$ and $\mathbf{S}_2$ are known in that $\mathbf{u}(t)$ contain feedforward, nonlinear feedback, and non-linear switching terms that make for inherent robustness. It is clear that $[\mathbf{g}(\mathbf{x}(t), \mathbf{z}(t))]$ must be invertible for all $[\mathbf{x}(t)\ \mathbf{z}(t)]$ in the range of motions contemplated and of rank equal to the number of controllers; that the system must be controllable; and it can be shown that the closed loop behavior on the sliding surface is characterized by poles (same as the number of independent controllers) at the origin in the error space; and that $\mathbf{S}_1$, $\mathbf{S}_2$ may be selected so that stable performance with desired bandwidth is also achieved.

SOLUTION BY SEPARATE AUTOPILOTS FOR SEPARATE SUBSYSTEMS

The foregoing analysis is, however not practical since in flight conditions as opposed to dynamic positioning of ROV's, there are often a smaller number of independent actuators than degrees of freedom. For instance, both pitch and heave modes are controlled by dive planes. Both sway and yaw are controlled by rudders. The choice of $\mathbf{S}_1 = \mathbf{I}$ is therefore not valid and $\mathbf{g}$ is rank deficient in these cases. We seek an alternative solution approach by separating the system into non-interacting (or lightly interacting) subsystems, grouping certain key motion equations together for the separate functions of steering, diving, and speed control. Other modes of response, such as roll, are commonly left passive - as is the case here. For dynamic positioning control we would return to the case of full rank for $\mathbf{g}$ and proceed as earlier outlined.

Restructuring, and linearizing equations (4) about a nominal flight path, we get for each subsystem,

$$d\mathbf{x}_i(t) / dt = \mathbf{A}_i\,\mathbf{x}_i(t) + \mathbf{b}_i\,u_i(t) + \mathbf{df}_i(\mathbf{x}_i(t),\mathbf{x}_j(t),\mathbf{u}_j(t),t)$$
$$\text{for } i = 1,..,4 \quad j = 1,..,4 \qquad (13)$$

and the $\delta\mathbf{f}_i$ represent non-linear and coupling terms as functions of the coupling motions $\mathbf{x}_j(t)$ and other controls $\mathbf{u}_j(t)$. In particular, let,

TABLE I
Table of subsystem states and inputs

Speed control states: $\mathbf{x}_1'(t) = [u(t)]$; $u_1(t) = n(t)$,
Steering system states: $\mathbf{x}_2'(t) = [v(t), r(t), \psi(t)]$; $u_2(t) = \delta_r(t)$,
Diving system states: $\mathbf{x}_3'(t) = [w(t), q(t), \theta(t), Z(t)]$; $u_3(t) = d_s(t)$,

and all others remain uncontrolled.

CONTROL PHILOSOPHY FOR THE THREE AUTOPILOTS

A philosophy of control which is derived by the particular choice of subsystem equations is that the steering system will be controlled by a heading command where the steering autopilot will be responsible for control of the heading errors; the diving system will be responsible for the depth and pitch errors and control to depth/pitch commands; and the speed system will control to speed commands. It should be pointed out that this control philosophy maps directly with the current practice in naval submarines. The conversion of commands for path following to a global location (X,Y,Z) will be accomplished by guidance laws such as the Line of Sight (LOS) method described later, and by others such as in Papoulias (1991).

With only a single control element active for each subsystem, each may be treated separately as a single input, multi-state (SIMO) system with its own single sliding surface definition. We proceed to define,

$$\sigma_1(t) = \mathbf{s}_1.\tilde{\mathbf{x}}_1(t)\ ; \quad \sigma_2(t) = \mathbf{s}_2.\tilde{\mathbf{x}}_2(t)\ ; \quad \sigma_3(t) = \mathbf{s}_3.\tilde{\mathbf{x}}_3(t);$$

SIMO DESIGN METHOD

For any subsystem where,

$$\dot{\mathbf{x}}(t) = \mathbf{A}\mathbf{x}(t) + \mathbf{b}u(t) + \delta\mathbf{f}(t)$$

and

$$\mathbf{x}(t) \in \Re^{n\times 1}; \mathbf{b} \in \Re^{n\times 1}; \mathbf{A} \in \Re^{n\times n};$$

if the pair $(\mathbf{A}, \mathbf{b})$ is controllable, and $[\mathbf{s}'\ \mathbf{b}]$ is nonzero, then it may be shown [see De Carlo et. al.(1988) and Utkin (1977) for a comprehensive tutorial], that the sliding surface coefficients are elements of the left eigenvector of the closed loop dynamics matrix $\mathbf{A}_c$ corresponding to a pole at the origin and the matrix $\mathbf{A}_c$ is given by,

$$\mathbf{s}'[\mathbf{A}_c] = 0;$$

where, $\mathbf{A}_c = [\mathbf{A}-\mathbf{bk}]$ and $\mathbf{k}$ is the gain vector that places the closed loop poles of the system at

$$\lambda_1 = 0, \text{ and } \lambda_i,\ i = 2,..,n$$

are selected for performance.

The resulting sliding control law including the estimate $\delta\hat{\mathbf{f}}(t)$ of the uncertain disturbances $\mathbf{df}(t)$ becomes,

$$u(t) = [\mathbf{s}'\mathbf{b}]^{-1}[-\mathbf{s}'\mathbf{A}\mathbf{x}(t) - \mathbf{s}'\delta\hat{\mathbf{f}}(t) + \mathbf{s}'\dot{\mathbf{x}}_{com}(t) - \eta\tanh(\sigma(t)/\phi)]$$

or

$$\mathbf{u}(t) = -\mathbf{k}\mathbf{x}(t) - [\mathbf{s}'\mathbf{b}]^{-1}\mathbf{s}'\delta\hat{\mathbf{f}}(t) + [\mathbf{s}'\mathbf{b}]^{-1}\mathbf{s}'\dot{\mathbf{x}}_{com}(t)$$
$$-[\mathbf{s}'\mathbf{b}]^{-1}\eta\tanh(\sigma(t)/\phi) \qquad (14)$$

The choice of the switching gain, $\eta(t)$ and the "boundary layer thickness" ϕ, is a design issue. Further details are given in Sur (1989), and Lienard (1990).

The excellent robustness attributed to the sliding control method can be clarified by recasting the closed loop equations of motion using (14) to get

$$\dot{\mathbf{x}}(t) = [\mathbf{A}-\mathbf{bk}]\mathbf{x}(t) + \dot{\mathbf{x}}_{com}(t) - \delta\hat{\mathbf{f}}(t) + \delta\mathbf{f}(t) -$$
$$\mathbf{b}[\mathbf{s}'\mathbf{b}]^{-1}\eta\tanh(\sigma(t)/\phi)$$

and since,

$$\dot{\sigma}(t) = s'(\dot{x}(t) - \dot{x}_{com}(t))$$

we get,

$$\dot{\sigma}(t) = -\eta \tanh(\sigma(t)/\phi) + s'[\delta f(t) - \delta\hat{f}(t)]$$

Thus so long as η is chosen to be 'large enough' to overcome the destabilizing effects of any disturbance mismatch, bounded stability of the errors is assured. In this case η is selected so that

$$\eta > \|s\| \left\| [\delta f(t) - \delta\hat{f}(t)] \right\| \qquad (15)$$

SPEED CONTROL AUTOPILOT

The longitudinal equation of motion, neglecting the effects of plane drag, is

$$\dot{u}(t) = -\alpha u(t)|u(t)| + \beta n(t)|n(t)| \qquad (16)$$

where,

$$\alpha = \frac{\rho L^2 C_d}{[2m + \rho L^3 X_{\dot{u}}]} \qquad \beta = \alpha u_0^2 / n_0^2 \quad C_d = 0.0034$$

and is linear in the modified square of the vehicle and propeller speeds.

The sliding surface for the speed control autopilot is thus first order and, without loss of generality, we can select $\sigma_1 = 1$ so that,

$$\sigma_1(t) = (u(t) - u_{com}(t)) = \tilde{u}(t) \qquad (17)$$

with the result that the control law in terms of the command for n(t) is found from,

$$\dot{\sigma}_1(t) = -\eta_1 \tanh(\sigma_1(t)/\phi_1)$$

giving,

$$n(t)|n(t)| = (\beta)^{-1}\{\alpha u(t)|u(t)| + \dot{u}_{com}(t) - \eta_1 \tanh(\sigma_1(t)/\phi_1)\} \qquad (18)$$

with n(t) equal to the signed square root of the right hand side of (18). Depending on the choice of ϕ_1, equation (18) is similar in form to a predictor / corrector control with a saturation in the error correction term. An integral of error component may be added to balance the unmodeled disturbances that cause speed changes if necessary.

STEERING AUTOPILOT

The linearized steering system dynamics are given by the third order system below with u_0 being the nominal vehicle speed.

$$\begin{aligned} m_1\dot{v}(t) - m_2\dot{r}(t) &= Y_1 u_0 r(t) + Y_2 u_0 v(t) + Y_3 \delta_r(t) \\ m_3\dot{v}(t) + m_4 r(t) &= N_1 u_0 r(t) + N_2 u_0 v(t) + N_3 \delta_r(t) \\ \dot{\psi}(t) &= r(t) \end{aligned} \qquad (19)$$

while the progression of vehicle position, not included in the autopilot system dynamics, is given by,

$$\begin{aligned} \dot{X}(t) &= u(t)\cos\psi(t) - v(t)\sin\psi(t) + u_{cx} \\ \dot{Y}(t) &= u(t)\sin\psi(t) + v(t)\cos\psi(t) + u_{cy} \end{aligned} \qquad (20)$$

The coefficients Y and N are given in Table II.

TABLE II

$Y_1 = 0.5\rho L^3 u_0 Y_{\dot{r}}$	$N_1 = 0.5\rho L^4 u_0 N_{\dot{r}}$
$Y_2 = 0.5\rho L^2 u_0 Y_v$	$N_2 = 0.5\rho L^3 u_0 N_v$
$Y_3 = 0.5\rho L^2 u_0^2 Y_{\delta_r}$	$N_3 = 0.5\rho L^3 u_0^2 N_{\delta_r}$

By inversion of the mass matrix, equations (19) may be expressed as,

$$\dot{x}_2(t) = A_2 x_2(t) + b_2 u_2(t) \qquad (21)$$

where,

$$A_2 = \begin{bmatrix} \begin{bmatrix} m_1 & m_2 \\ m_3 & m_4 \end{bmatrix}^{-1} \begin{bmatrix} Y_1 & Y_2 \\ N_1 & N_2 \end{bmatrix} & \begin{matrix} 0 \\ 0 \end{matrix} \\ \begin{matrix} 0 & 0 \end{matrix} & 1 \end{bmatrix} \quad b_2 = \begin{bmatrix} \begin{bmatrix} m_1 & m_2 \\ m_3 & m_4 \end{bmatrix}^{-1} \begin{bmatrix} Y_3 \\ N_3 \end{bmatrix} \\ 0 \end{bmatrix} \qquad (22)$$

or, in more detail as,

$$\begin{bmatrix} \dot{v}(t) \\ \dot{r}(t) \\ \dot{\psi}(t) \end{bmatrix} = A_2 \begin{bmatrix} v(t) \\ r(t) \\ \psi(t) \end{bmatrix} + b_2 \delta_r(t) ; \quad A_2 \in \Re^{3\times 3}; \; b_2 \in \Re^{3\times 1} \qquad (23)$$

Defining the sliding surface for steering as

$$\sigma_2(t) = s_{21} v(t) + s_{22}[r(t) - r_{com}(t)] + s_{23}[y(t) - y_{com}(t)], \qquad (24)$$

the steering control law results in,

$$\delta_r(t) = k_{21} v(t) + k_{22} r(t) + k_{23} \dot{r}_{com}(t) + \eta_r \tanh(\sigma_2/\phi_2) \qquad (25)$$

Notice that in the above, the heading error term is only included in the non-linear switching term, while the linear feedback of v(t) and r(t) act only to stabilize the sway / yaw dynamics. The heading rate, $r_{com}(t)$, and $\dot{r}_{com}(t)$ are set to zero here although in rate command maneuvers they should be included in the control law. $v_{com}(t)$ is not practical to include. Further details of the speed and steering autopilots are given in Lienard (1990).

DIVING AUTOPILOT

The linearized diving system dynamics including the significant terms but ignoring the cross products of inertia and their effects are given by the system of equations,

$$[I_{yy} - 0.5\rho L^5 M_{\dot{q}}]\dot{q}(t) =$$

$$[0.5\rho L^4 M_q u_0] q(t) + [0.5\rho L^3 M_w u_0] w(t) + [0.5\rho L^3 M_\delta u_0^2]\delta_s(t)$$

$$-[z_G W - z_B B]\sin\theta(t) - \{[0.5\rho L^4 M_{\dot{w}}]\dot{w}(t) - [mz_G] w(t) q(t)\}$$

$$\dot{\theta}(t) = q(t)$$

$$\dot{Z}(t) = -u_0 \sin\theta(t) + w(t)\cos\theta(t)$$

In the above, the influence of w(t), which may be significant in some vehicles, is in fact small in this case; perhaps because of the rectangular cross section, and has also been neglected. Ignoring w(t), the diving model reduces to a three state model involving q(t), θ(t) and Z(t), with uncertain disturbances. The sliding surface for the diving autopilot ignoring any non zero command for pitch for now, then becomes

$$\sigma_3(t) = s_{31} q(t) + s_{32}[q(t) - q_{com}(t)] + s_{33}[Z(t) - Z_{com}(t)], \qquad (26)$$

$$\delta_s(t) = k_{31} q(t) + k_{32}\theta(t) + k_{33}\dot{q}_{com}(t) + \eta_s \tanh(\sigma_3/\phi_3) \qquad (27)$$

Externally to the computation of $\delta_s(t)$, it is necessary to limit commands for all control surface strokes to a value of 0.4 radians in order to prevent stall. Although the vehicle has eight independent control surfaces, upper and lower rudders are driven from the same rudder command and at the present time, bow and stern rudders are also driven from the same command with opposite polarity. Stern planes and bow planes are likewise commanded equally with opposite polarity. No attempt at this stage has been made to examine optimization of control effort distribution to reduce stall, or to control local angle of attack at any surface, even though certain experimental evidence exists to indicate the desirability of doing so.

VEHICLE CHARACTERISTICS

The vehicle design details have appeared elsewhere (Healey and Good 1992, Good, 1989), and will not be repeated except to say that the vehicle displaces 385 lbs. has a length dimension of approximately 2.15 meters, is supplied with lead/acid gel batteries for a test duration of about two hours, is completely autonomous with respect to power and control; is preprogrammed to execute a defined mission, has an internal suite of sensors that includes a 3-axis rate gyro system, a directional gyro with a flux-gate compass, a vertical gyro, a paddle wheel speed sensor, a pressure cell depth sensor, 4 sonar range sensors controlled by the central processor each with return processing at the local level interfaces through the A/D card, independent shaft speed sensors and controllers for each of two propulsion motors, has a GESPAC control computer with a Motorola 68030 25 MHz. processor, 2 Mb. RAM and A/D and D/A interface cards, a parallel interface card, and is programmed with control code in 'C' language. The vehicle's purpose is as a testbed for the development of intelligent control systems in mobile undersea robotics applications. It is nominally ballasted to be neutrally buoyant and to float level with a small (1": 2.5 cm) Z_B/Z_G separation for statically stable roll and pitch.

MANEUVERING RESPONSE: OVAL TRACK

Initial plans for testbed missions were to perform oval track runs in the NPS swimming pool. A series of missions were planned where the vehicle, operating under closed loop speed control, closed loop diving and steering control, followed a path with switch points defined at predetermined times at which heading commands were incremented from 0 to 180 to 360 degrees. In this way, the walls of the pool were avoided. This class of test run is helpful to identify the essential characteristics of the autopilot systems and has provided some interesting results shown in the series of Figures 2-5. Other runs including figure of eight, zig-zag, and spiral maneuvers have been completed. In Figure 2 the pertinent steering response variables are shown, Figure 3 gives the corresponding diving variables and Figure 4 shows the vehicle speed response. The path, as identified by dead reckoning ignoring side slip errors, is shown in Figure 5. Many other runs have been made recently and the results here will show a comparison of sliding mode controllers with more standard designs, bottom following performance with a downward looking sonar, and way point following in a figure eight maneuver.

Steering Response

The steering response is shown in Figure 2. The figure shows the behavior of a PD steering controller given by,

$$\delta_r(t) = K_r r(t) + K_\psi(\psi(t)-\psi_{com}(t))$$

where the rudder command signal time history is shown together with the corresponding yaw rate and heading angle. In the first thirty seconds, the vehicle is accelerating to speed, diving to depth, and controlling to the desired heading. At thirty seconds, the command to turn is entered and the response in the turn is clearly seen. The performance of the controller, however, is not elucidated when the turn is entered because the rudders are saturated. It is the control when the vehicle exits from the turn during the period 50 - 70 seconds that is key. The controller represents a balance between responsiveness and stability in controlling the turn and has been designed to have somewhat higher proportional gain than would be necessary if tight turns were not needed. The corresponding heading angle is clearly shown in Figure 2. The oscillatory part of the yaw rate during the period 35 - 45 seconds is possibly generated by inertial cross-coupling that potentially exists between the pitch / yaw modes although nominally assumed to be negligible. Later experiments

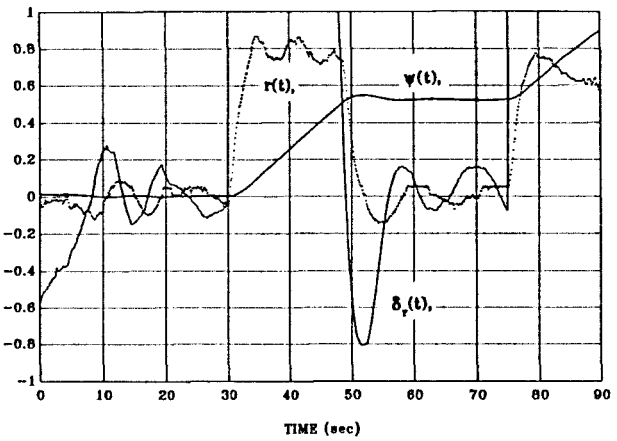

Figure 2

$\delta_r(t)$, r(t), $\psi(t)$, versus Time. [Run 7-8-91-5]; Oval Track Run; Combined Diving, Steering, and Speed Control; Standard Control Laws; Scaled as $\delta_r(t)/0.4$(rad), r(t)/0.2(rad/sec), $\psi(t)/6.0$(rad)

with tighter control suppressed this phenomenon to a large degree. This is evidence that high gain robust controllers are indeed needed for these separate autopilots in compensating for the induced mode coupling.

Diving Response

The diving response is indicated in Figure 3. There is an initial flurry of dive plane control action as the vehicle accelerates to speed and goes below the water surface. The initial launch is on the surface and the transition to depth is smooth but initially the vehicle speed is slow and the control is less effective than at the nominal running speed about 2 ft/sec. (0.61 meters/sec.). The pitch rate and angle are shown. The pitch angle reaches 0.2 radians then is reduced quickly and the nominal depth of 2 feet (0.61 meters) is achieved. At the end of the test run, the mission calls for a depth change to surface as indicated at the time of 75 seconds. The pitch control law for which the results are shown was a three state proportional law without the nonlinear term, given by,

$$\delta_s(t) = K_q q(t)+K_\theta\theta(t)+K_z\,[Z(t)-Z_{com}(t)]$$

Speed Response

The vehicle speed control was provided by a control law given by (18) including an integral term, where with abuse of notation,

$$n_{com}(t) = (u_0/n_0)u_{com}(t) + K_1 e(t) + \sum_{i=1}^{10} e_{k-i}\ .$$

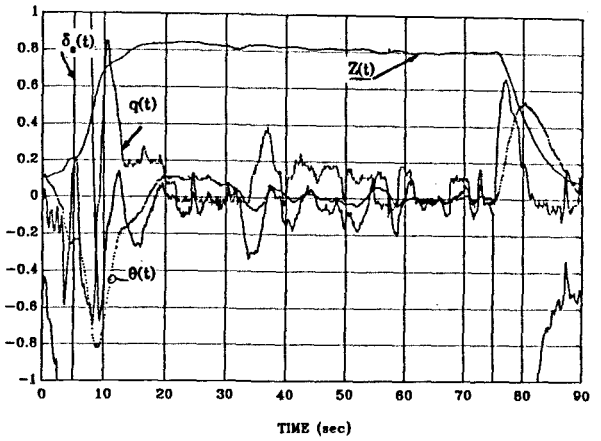

Figure 3

$\delta_s(t)$, q(t), θ(t), and Z(t) versus Time. [Run 7-8-91-5]; Oval Track Run; Combined Diving, Steering, and Speed Control; Standard Control Laws; Scaled as $\delta_s(t)/0.4$ (rad), q(t)/0.08(rad/sec), θ(t)/0.25 (rad), Z(t)/2.5 (ft.)

The integral term as a sum over the last ten points was present to help in maintaining speed during the turn where the large centrifugal force and the added plane drag causes significant loss of speed. The response in Figure 4 shows the output from the paddle wheel sensor indicating good acceleration followed by an overshoot at 2.5 ft/sec with a controlled speed reduction during the period 20 - 30 seconds. The speed reduction during 30 - 50 seconds is the effect of the added drag terms which would be much larger without the corresponding increase in propeller speed not shown. (Shown in later runs). The speed gain during the period 50 - 70 is the result of the vehicle coming out of the turn and the speed controller taking over in stabilizing to the set point of 2 ft./sec. (0.61 meters /sec.).

The path obtained by dead reckoning using the paddle wheel speed sensor and the heading gyro output but neglecting side slip errors is given in Figure 5. Recognizing the limitations of the accuracy of this navigation scheme, we have found the results sufficient to guide the vehicle without a collision with the pool walls.

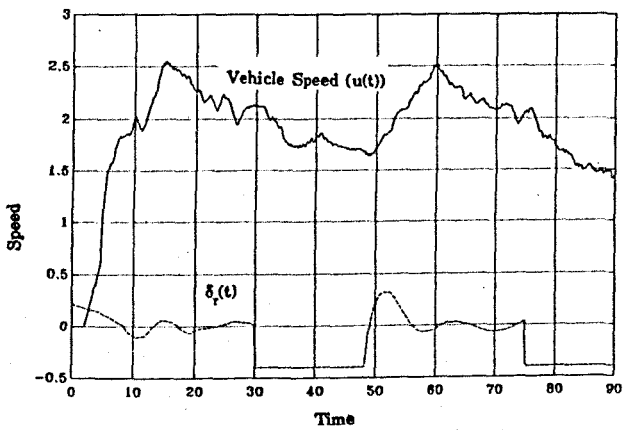

Figure 4

Vehicle Speed (u(t)) versus Time. [Run 7-8-91-5]; Oval Track Run; Combined Diving, Steering, and Speed Control; Standard Control Laws

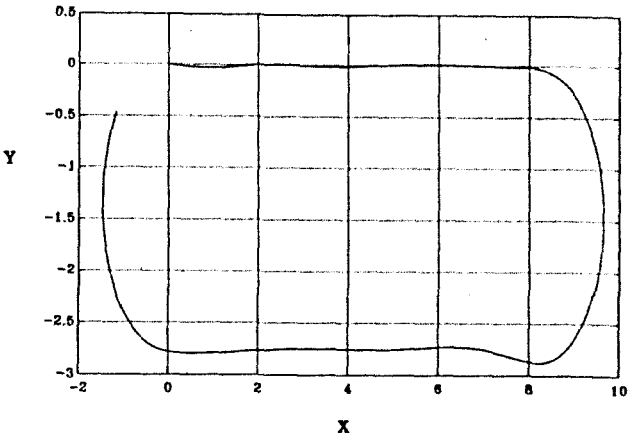

Figure 5

Vehicle Path versus Time. [Run 7-8-91-5]; Oval Track Run; Combined Diving, Steering, and Speed Control; Standard Control Laws; X and Y expressed in Vehicle Lengths

WAY POINT GUIDANCE BY LINE OF SIGHT

Vehicle autonomous guidance is most simply accomplished by a heading command to the vehicle's steering system to approach the line of sight between the present position of the vehicle and the way point to be reached. In missile guidance this is related to 'proportional navigation'. The difference in guiding AUV's is that the vehicle response is slow compared to the rates of change in command unless the way point is many vehicle lengths away. Separation of guidance and autopilot functions may not always produce stable results underwater. Notwithstanding, we define the line of sight (LOS) to be the horizontal plane angle given by,

$$\psi_{com} = \tan^{-1}\left[\frac{(Y_k - Y(t))}{X_k - X(t)}\right]$$

in which the $[X_k, Y_k]$ are way points stored in the vehicle's mission planner. Care must be taken to keep the proper quadrant in mind when programming the guidance law. The decision as to whether the way point has been reached is made on the basis of whether the vehicle lies within a 'ball of acceptability', r_0 defined around the particular way point. Namely, if, for some distance, r_0, an acceptable zone around the way point, $[X_k(t), Y_k(t), Z_k(t)]$, the vehicle location [X(t), Y(t), Z(t)] are such that,

$$\rho^2(t) = [Y_k - Y(t)]^2 + [X_k - X(t)]^2 + \lambda[Z_k - Z(t)]^2 < \rho_0^2 \qquad 0 < \lambda < 1$$

the above condition triggers the selection of the next way point. If, on the other hand, the condition that dρ/dt goes from negative to positive without the above being met then the way point is not reached. At this juncture, the guidance law must contain logic that will either hold the current way point, directing the vehicle to circle, or the next way point could be entered, depending on a mission planning decision. λ is a parameter relating to the importance of including depth dimension in the acquisition of the way point. In this section, vehicle way point control is examined in experiment using the autopilots described above combined with the LOS guidance. The assumption is made that vehicle speed control is obtained from a separate speed command for each separate leg of a transit mission, although that could be accomplished also by an on line speed command as a function of distance to go and the time to go if a desired time is also associated with each way point. The ability of the LOS method to acquire way points is illustrated by the series of results given in Figures 6

- 9. In Figure 6, the steering response variables are shown with rather oscillatory swings that are characteristic of commands changing as way points are reached and subsequent points entered into the controller. The diving performance is given in Figure 7 where a commanded depth of 2 ft again was used. Figure 8 shows the speed controller response as the vehicle is accelerated and slowed by the turning activity. In Figure 8, the propeller speed command is shown as well as the vehicle speed response from the paddle wheel sensor. Separate experiments, not described here, have determined that the response of the inner loop for the control of motor speed to motor speed commands is fast and has negligible lags in this application. Figure 9 shows that each way point was acquired with excellent precision even though the global locations of those way points may have been uncertain. In other words, the autopilot functions drove the vehicle to the locations that the vehicle 'thought' it had to meet.

What we see is a vehicle that is capable of tight turns; its steering and diving systems are stable under conditions of combined maneuvering at speeds that are changing; and planned paths, in terms of way points, can be followed with precision consistent with the limits of the vehicle's turning capability.

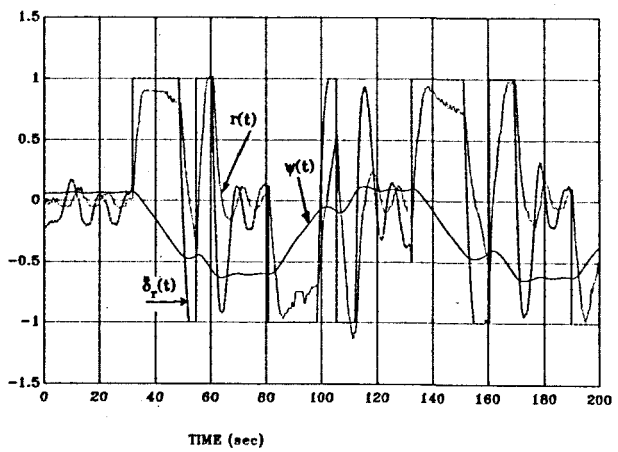

Figure 6
Figure Eight Run; Vehicle Steering Response. [Run 7-29-91-5]; Combined Diving, Steering, and Speed Control; Standard Control Laws; $\delta_r(t)$, r(t), ψ(t), versus Time.Shown During the Run

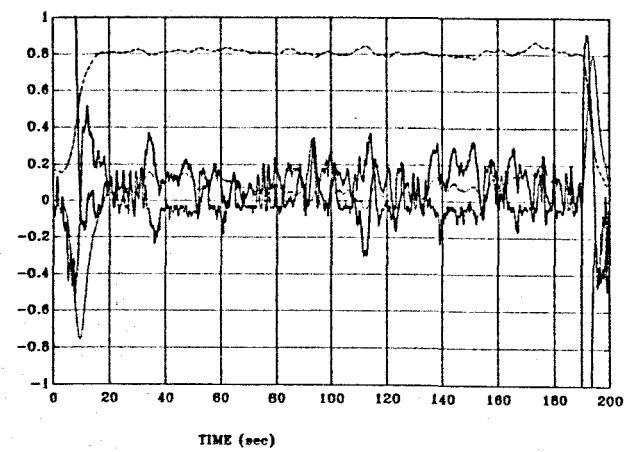

Figure 7
Figure Eight Run; Vehicle Diving Response. [Run 7-29-91-5]; Combined Diving, Steering, and Speed Control; Standard Control Laws; Plot As in Figure 3

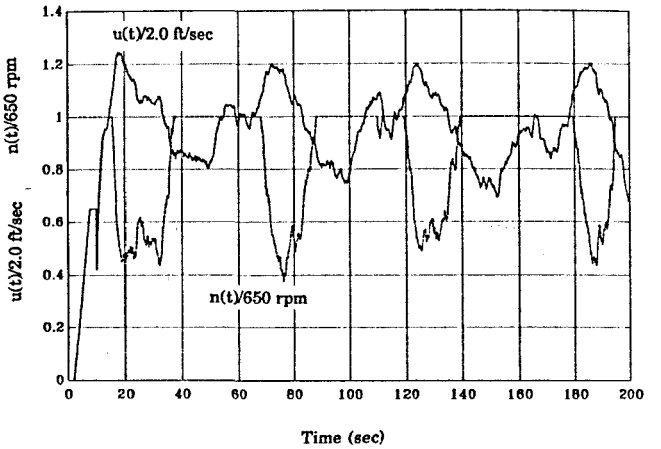

Figure 8
Figure Eight Run; Vehicle Speed (u(t)) versus Time. [Run 7-29-91-5]; Combined Diving, Steering, and Speed Control; Standard Control Laws. Normalized Plot u(t)/2.0 ft/sec. n(t)/650 rpm

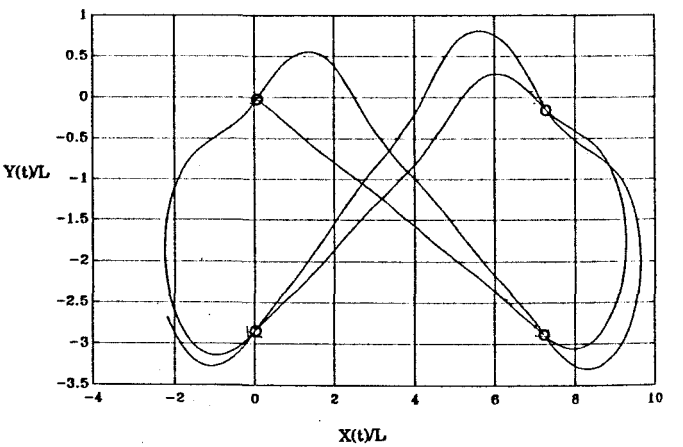

Figure 9

Figure Eight Run; Vehicle Path [Run 7-29-91-5]; Combined Diving, Steering, and Speed Control; Standard Control Laws. Way Points Shown. X(t)/L versus Y(t)/L

SLIDING MODE COMPARED

The performance of sliding mode control has been compared in a series of runs using the same oval path as in the first series with the steering control law,

$$\delta_r(t) = k_{21}v(t)+k_{22}r(t)+k_{23}\dot{r}_{com}(t)+\eta_r\tanh(\sigma_2/\phi_2)$$

In Figures 10a and 10b, three controller's results are superimposed with the rudder responses shown in Figure 10a, and the corresponding yaw rate responses shown in Figure 10b. Each shows the effect of increasing nonlinear gains. The effect on the yaw rate response out of the turn is not as strong as thought and increasing gain appears to increase the levels of activity on the control surfaces. However, the overall response is very rapid and much improved over the initial PD controller. It is believed that the sliding mode control is easy to implement and even easier to tune in the field as only one parameter needs to be modified to adjust the speed of the controller from slow to fast and stability is not compromised.

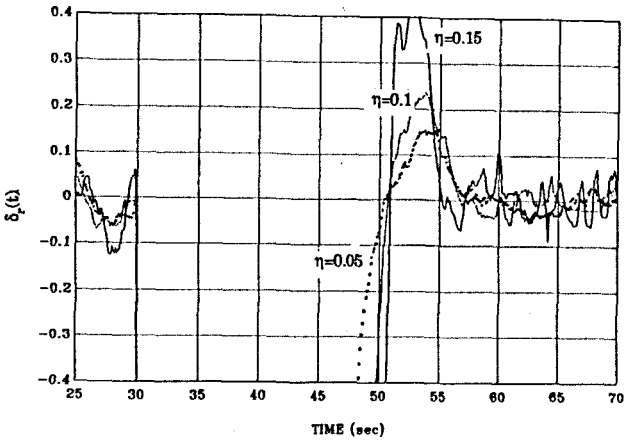

Figure 10 a
Oval Track Run; Vehicle Rudder versus Time. [Run 9-9-91-3-5]; Sliding Mode Steering Control Laws; Varying Nonlinear Gains η=[0.05, 0.1, 0.15]

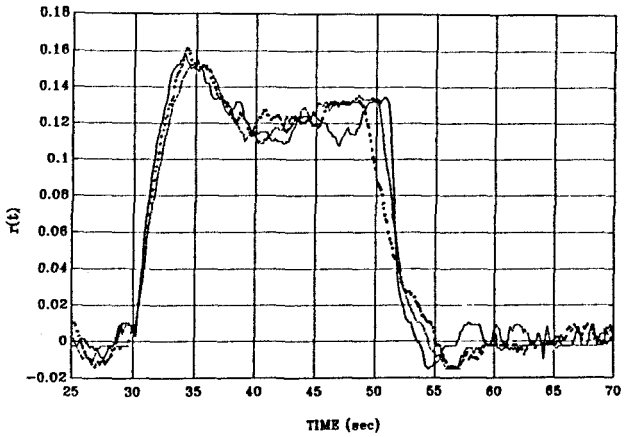

Figure 10 b
Oval Track Run; Vehicle Yaw Rate versus Time. [Run 9-9-91-3-5]; Sliding Mode Steering Control Laws; Varying Nonlinear Gains η=[0.05, 0.1, 0.15]

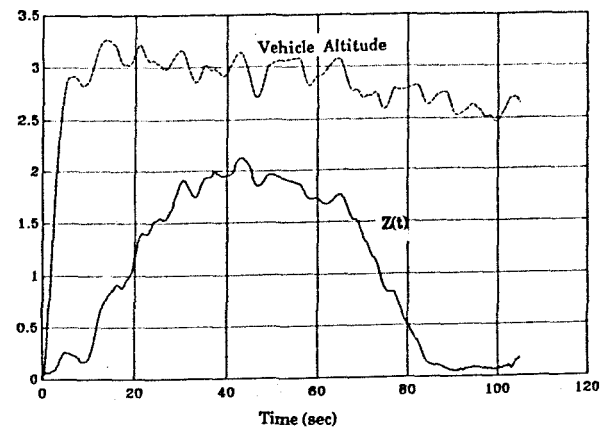

Figure 11
Oval Track Run; Bottom Following; Water Depth versus Time. [Run 5-10-91-5]; Combined Diving, Steering, and Speed Control

BOTTOM FOLLOWING

Incorporation of a downward looking sonar (Datasonics PSA 900) into the depth control system has allowed a test series for altitude control and also using the vehicle depth sensor, a determination of the water column height around the pool. For the basic oval loop, Figure 11 shows the result of the control to a fixed height above bottom, and the attendant measurement of the vehicle depth.

CONCLUSIONS

In conclusion, the use of sliding mode methods has been shown to provide easy to implement performance for underwater vehicle autopilots. Good performance is obtained when controls are designed separately for speed control, steering and diving activity. The method is generally suitable for a wide variety of non-linear control problems, although for flight conditions, is simplified by using a linearized model for the sliding surface coefficient design. Experimental results using the NPS AUV II testbed vehicle have illustrated the validity of the vehicle's motion control design. More precision in path following could result from more refined path planning algorithms taking into account the vehicle's turning properties and side slip behavior. Combined control using motion sensors and sonar signals is not easy to accomplish and the attendant noise on the sonars used is not satisfactory for providing precise positioning control. Further investigation of the dynamic performance of propeller propulsion is certainly warranted. At the present time, high precision in motion control needs further understanding particularly in the transition from cruise to hover modes.

ACKNOWLEDGEMENTS

The authors wish to recognize the financial support of the Naval Postgraduate School Direct Research Fund under the technical sponsorship of the Naval Surface Warfare Center, White Oak Laboratories and the Office of Naval Technology for the AUV project at NPS.

REFERENCES

Abkowitz, M. A., "Stability and Motion Control of Ocean Vehicles ", *M.I.T. Press*, 1969.

Cristi, R., Papoulias, F. A., Healey, A.J., "Adaptive Sliding Mode Control of Autonomous Underwater Vehicles in the Dive Plane", *IEEE Journal of Oceanic Engineering*, Vol. 15, No. 3, 1991, pp 462-470

Dand, I. W., Every, M. J.,"An Overview of the Hydrodynamics of Umbilical Cables and Vehicles- Parts I and II" *Proceedings of Subtech '83*, Society for Underwater Technology, London, 1983 pp 525-562

De Carlo, R. A., Zak, S. H., Mathews, G. P., "Variable Structure Control of Non-Linear Multivariable Systems: A Tutorial " *Proc. IEEE* v 76, n 3, March 1988, pp 212-232

Dobeck, G. J., Watkinson, K. W., Freeman, E. H., "Navigation, Guidance, and Control of an Autonomous 30-Foot Model Submarine" *Report No NCSC TR 370-82*, Naval Coastal Systems Center, Panama City, FA. June 1982

Dougherty, F., Woolweaver, G., " At Sea Testing of an Underwater Vehicle Flight Control System" *Proceedings of the AUV 90*, IEEE Catalog No. 90CH2856-3 1990, pp 51-59

Fossen, T.I.,"Nonlinear Modeling and Control of Underwater Vehicles", Dr.Ing. Thesis, Norwegian Institute of Technology, Trondheim, 1991

Gertler, M., and Hagen, G. R., "Standard Equations of Motion For Submarine Simulations," *NSRDC Report No. 2510* 1967.

Goheen, K. R., Jefferys, E. R., Broome, D. R., "Robust Self Designing Controllers for Underwater Vehicles" *Trans. ASME Journal of Offshore Mechanics and Arctic Engineering*, Vol.109, May 1987, pp 170-178

Good, M., "Design and Construction of a Second Generation Autonomous Underwater Vehicle" *MS. Degree Thesis. Naval Postgraduate School* December 1989

Gueler, G. F., "Modelling, Design and Analysis of an Autopilot for Submarine Vehicles," *International Shipbuilding Progress*, Vol. 36, No. 405, 1989, pp 51-85

Healey, A. J., Good, M.,"The NPS AUV II Autonomous Underwater Vehicle Testbed: Design and Experimental Verification" ASNE *Naval Engineers Journal* May, 1992

Healey, A.J., "Model Based Maneuvering Controls for Autonomous Underwater Vehicles" *ASME Transactions Journal of Dynamic Systems Measurement and Control*, to appear 1992

Humphries, D.,"Dynamics and Hydrodynamics of Ocean Vehicles," *IEEE OCEANS '81 Conference Proceedings* Vol. 1.,1981, pp 88-91

Lewis, D.J., Lipscomb,J. M.,Thompson, P.G.,"The Simulation of Remotely Operated Underwater Vehicles" *Proceedings of ROV '84*. The Marine Technology Society, San Diego, CA. 1984 pp 245-252

Lienard, D. " Sliding Mode Control for Multivariable AUV Autopilots" *Mechanical Engineer's Thesis. Naval Postgraduate School* June 1990

Lindgren, A. G., Cretella, D. B., Bessacini, A. F.,"Dynamics and Control of Submerged Vehicles" *Trans. Instrument Society of America* Vol. 6, Issue 4, Dec. 1967, pp 335-346

Milliken, G. L., "Multivariable Control of an Underwater Vehicle", *M.S. Thesis*, MIT, Cambridge, Mass., 1984

Papoulias, F. A., "Stability Considerations of Guidance and Control Laws for Autonomous Underwater Vehicles in the Horizontal plane" *Proceedings of the 7th Symposium on Unmanned,Untethered, Submersible Technology*, University of New Hampshire, Durham, New Hampshire, September 23-25 1991.

Richards, R.J., Stoten, D.P., "Depth control of a Submersible Vehicle" *International Shipbuilding Progress* Vol. 28 No 318 Feb. 1981, pp 30-39

Russel, G. T., Bugge, J., "Adaptive Estimator for the Automatic Guidance of an Unmanned Submersible' *Proc. Inst. Elect. Eng.*, Vol.128, pt D.,No. 5 pp 223-226 Sept. 1981

Ruth, M. J., Humphreys, D.E., "A Robust Multivariable Control System For Low Speed UUV Operation", *Proceedings of the AUV 90*, IEEE Catalog No. 90CH2856-3 1990, pp 88-91

Smith, N.S., Crane, J.W., and Summey, D. C., "SDV Simulator Hydrodynamic Coefficients ", *NCSC Report No. TM-231-78* June 1978.

Sur, J. N., "Preliminary Investigations of Variable Structure Controls for the NPS Model 2 AUV" *M.S.Thesis Naval Postgraduate School*, Monterey, Calif. June 1989

Utkin,V.I., " Variable Structure Systems with Sliding Modes " *IEEE Transactions on Automatic Control* April 1977 pp 212-222

Yoerger, D. R., Slotine, J. J. E., "Robust Trajectory Control of Underwater Vehicles," *IEEE Journal of Oceanic Engineering*, Vol. 10, No. 4, October 1985, pp 462-470.

Yoerger, D. R., Neuman, J.B., Slotine, J. J. E., "Supervisory Control Systems for the JASON ROV" *IEEE Journal of Oceanic Engineering*, Vol. 11, No. 3, 1986, pp 392-400.

Yoerger, D.R., Cooke, J.G., Slotine, J.J.E., "The Influence of Thruster Dynamics on Underwater Vehicle Behavior and Their Incorporation into Control System Design" *IEEE Journal of Oceanic Engineering*, Vol. 15, No. 3, 1991, pp 167-178

Young, D. B., "Model Investigation of the Stability and Control Characteristics of the Contract Design for the Deep Submergence Rescue Vehicle (DSRV)," *Report No. 3030, David Taylor Research Center*, Bethesda, MD. April 1969